Rev. Roum. Sci. Techn.– Électrotechn. et Énerg.
Vol. **62**, *2*, pp. 197–202, Bucarest, 2017

OUTPUT POWER CONTROL OF A VARIABLE WIND ENERGY CONVERSION SYSTEM

KARIMA BOULÂAM, AKKILA BOUKHELIFA

Key words: Wind energy conversion system (WECS), Maximum power point tracking (MPPT), Doubly fed induction generator (DFIG), Sliding mode control.

In this paper, the control of a variable wind energy conversion system (WECS) based on a doubly fed induction generator (DFIG) is proposed. The DFIG control structure contains rotor currents and stator powers loops where proportional-integral (PI) controllers are used. This control could be obtained by applying the DFIG's active and reactive powers decoupling strategy based on stator flux orientation method. For the wind turbine, a nonlinear controller based on the sliding mode theory is proposed to maximize the extracted power. This controller works in the partial load region. Another control algorithm has been used to work in full load region. It controls the generator output power via the pitch angle so as not to exceed the rated power of the system. The proposed MPPT and pitch control algorithms provide good static and dynamic performances. The validity of the proposed strategies is analyzed throw simulation.

1. INTRODUCTION

Wind energy is becoming one of the most important renewable sources. Many studies [1–8] are oriented toward this type of energy production in the aim to make it more efficient.

Variable speed wind turbines are widely used in this field owing to their ability to maximize wind power extraction [1–8]. The one analyzed in this paper is based on a doubly fed induction generator (DFIG). This machine presents different advantages [2, 3] such as: operating in a wide range of speed (± 33 % around the synchronous speed), generating a constant frequency active power and the possibility of the generated active and reactive power to be controlled independently. In addition, such a system results in lower converter costs (typically 25 % of total system power) and power losses compared to a system based on a fully fed synchronous generator with full rated converter.

Using an appropriate control algorithm could improve the wind power efficiency. Linear and non-linear controls are used by authors [1–8]. A nonlinear control has been adopted in this paper. It is more suitable for non-linear systems, such as the wind turbine model. This control is based on sliding mode theory.

In Section 2, the structure of the proposed WECS is presented. In Section 3, the generator modeling and the control of its active and reactive powers are given. The wind turbine model is presented in Section 4. In Section 5, we explain first the maximum power point tracking (MPPT) technique then the generator speed control scheme is given, after what a sliding mode algorithm is proposed to be applied to the speed control model. In Section 6, a pitch control scheme is proposed to be applied in full load region. Finally, analyzed results show the good behaviors given by the use of both the sliding mode and the pitch control algorithms, Section 7.

2. PRESENTATION OF WIND ENERGY SYSTEM CONVERSION

The wind energy conversion system used is represented in Fig. 1. It is based on a doubly fed induction generator (DFIG) which is a wound rotor induction generator connected to the wind turbine rotor through a gearbox.

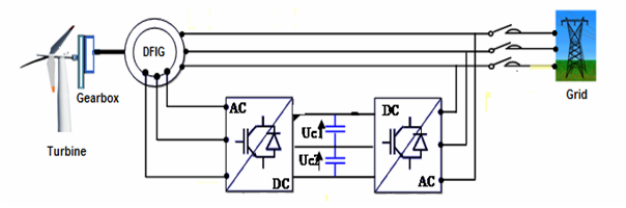

Fig. 1 – Schematic diagram of the wind energy conversion system.

The stator winding is directly coupled to the grid when the rotor winding is connected to the grid via a bidirectional pulse width modulation (PWM) power converter. This converter is constituted by a neutral point clamped (NPC) structure three-level inverter associated with a NPC three level rectifier converter linked by a two capacitors dc bus [9]. This power converter decouples the electrical grid frequency and the mechanical rotor frequency, thus enabling variable speed wind turbine generation. The stator's powers are controlled by the rotor's currents. The MPPT technique with the control of the generator speed using a nonlinear algorithm is realized.

3. MODELING AND CONTROL OF THE DFIG

The dynamic model of the generator written in a synchronously rotating frame *d–q* [2, 4, 7] is given by the following equations system:

$$\begin{cases} V_{sd} = R_s I_{sd} + \dfrac{\mathrm{d}}{\mathrm{d}t}\Phi_{sd} - \omega_s \Phi_{sq} \\ V_{sq} = R_s I_{sq} + \dfrac{\mathrm{d}}{\mathrm{d}t}\Phi_{sq} - \omega_s \Phi_{sd} \end{cases}, \tag{1}$$

$$\begin{cases} V_{rd} = R_r I_{rd} + \dfrac{\mathrm{d}}{\mathrm{d}t}\Phi_{rd} - (\omega_s - \omega)\Phi_{rq} \\ V_{rq} = R_r I_{rq} + \dfrac{\mathrm{d}}{\mathrm{d}t}\Phi_{rq} + (\omega_s - \omega)\Phi_{rd} \end{cases}, \tag{2}$$

$$\begin{cases} \Phi_{sd} = L_s I_{sd} + M I_{rd} \\ \Phi_{sq} = L_s I_{sq} + M I_{rq} \end{cases}, \quad \begin{cases} \Phi_{rd} = L_r I_{rd} + M I_{sd} \\ \Phi_{rq} = L_r I_{rq} + M I_{sq} \end{cases}, \tag{3}$$

Instrumentation Laboratory, Faculty of Electronics and Computing, University of Sciences and Technology Houari Boumediene, PO Box 32 El Alia, Bab Ezzouar 16111, Algiers, Algeria, E-mail: kboulaam@yahoo.fr; aboukhelifadz@yahoo.fr

$$T_{em} = p\frac{M}{L_s}\left(\Phi_{sq} I_{rd} - \Phi_{sd} I_{rq}\right) \tag{4}$$

$$\begin{cases} P_s = V_{sd} I_{sd} + V_{sq} I_{sq} \\ Q_s = V_{sq} I_{sd} - V_{sd} I_{sq} \end{cases} \tag{5}$$

where: s, (r) is stator (rotor) index; d, (q) is direct (quadrature) synchronous reference frame index; V (I) is voltage (current); Φ is flux; P_s (Q_s) is stator's active (reactive) power; T_{em} is electromagnetic torque; R is resistance; L (M) is inductance (mutual inductance); ω, (ω_s) is angular speed (synchronous speed); p is pole pair number.

To be able to easily control the wind turbine power generation, we will realize an independent control of the stator active and reactive powers.

The control system adopts the oriented flux strategy defined in the synchronous d–q frame fixed to the stator according to eq (6).

$$\begin{cases} \Phi_{sd} = \Phi_s \\ \Phi_{sq} = 0 \end{cases}. \tag{6}$$

In addition, the electric network can be considered as an infinite energy source so that the stator's flux vector is considered as a constant, and the voltage drop caused by the stator resistance is negligible comparing to the stator voltage value [2]. With these assumptions, the mathematic model of DFIG in the synchronous reference (d-q) frame linked to the stator's flux can be written as follows:

$$\begin{cases} V_{sd} = 0 \\ V_{sq} = V_s = \omega_s \Phi_{sd} \end{cases}, \tag{7}$$

$$\begin{cases} V_{rd} = R_r I_{rd} + \sigma L_r \dfrac{\mathrm{d}}{\mathrm{d}t} I_{rd} - s\omega_s \sigma L_r I_{rq} \\ V_{rq} = R_r I_{rq} + \sigma L_r \dfrac{\mathrm{d}}{\mathrm{d}t} I_{rq} + s\omega_s \sigma L_r I_{rd} + s\dfrac{M}{L_s} V_s \end{cases}, \tag{8}$$

$$T_{em} = -p\frac{M}{L_s}\Phi_{sd} I_{rq}, \tag{9}$$

$$\begin{cases} P_s = -V_s \dfrac{M}{L_s} I_{rq} \\ Q_s = -V_s \dfrac{M}{L_s} I_{rd} + \dfrac{V_s^2}{\omega_s L_s} \end{cases}, \tag{10}$$

with: σ – leakage coefficient ($\sigma = 1 - M^2/(L_s L_r)$); s – slip.

According to (10), we can see that the active and reactive powers of the stator P_s and Q_s can be controlled by the rotor currents I_{rq} and I_{rd} respectively. This control is made via the rotor voltage components V_{rq} and V_{rd} (8).

The DFIG control structure (Fig. 2) contains two cascaded control loops (inner and outer) for each axis d and q. The inner loop controls the current and the outer one the power. PI controllers are used to control both rotor currents and stator powers.

The desired active power reference P_{sref} corresponds to the maximum power point given by the generator speed regulator. Q_{sref} is imposed equal to zero, in order to operate at unitary power factor. The currents references will be given by the powers' controllers.

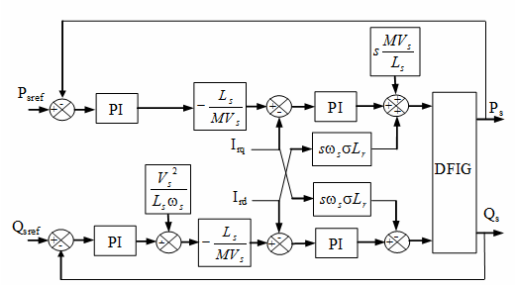

Fig. 2 – Control scheme of the generator powers.

4. WIND TURBINE MODELING

The aerodynamic power developed by a wind turbine is given by the following expression [2, 3, 6, 7]:

$$P_{aer} = \frac{1}{2}\cdot C_p(\lambda,\beta)\cdot\rho\cdot\pi\cdot R^2\cdot v^3, \tag{11}$$

$$\lambda = \frac{R\cdot\Omega_{turb}}{v}, \tag{12}$$

with: ρ – air density; v – wind speed; C_p – power coefficient; β – blade pitch angle; λ – tip-speed ratio; R – radius of rotor, Ω_{tutb} – the turbine rotor speed.

The power coefficient C_p defines the aerodynamic efficiency of the wind turbine rotor. It is represented by various approximation expressions. In this paper, C_p is expressed [1] by eq. (13)

$$\begin{cases} C_p(\lambda,\beta) = 0.5176\left(\dfrac{116}{\lambda_i} - 0.4\beta - 5e^{-\frac{21}{\lambda_i}}\right) + 0.0068\,\lambda \\ \dfrac{1}{\lambda_i} = \dfrac{1}{\lambda + 0.08\,\beta} - \dfrac{0.035}{\beta^3 + 1} \end{cases}. \tag{13}$$

The mechanical equation of the shaft, including both turbine and generator masses, is given by eq. (14).

$$J_t\frac{\mathrm{d}\,\Omega}{\mathrm{d}t} = T_g - T_{em} - f_t\Omega, \tag{14}$$

where J_t and f_t are totals moment of inertia and viscous friction coefficient appearing at the generator side; T_g is the gearbox torque; T_{em} is the electromagnetic torque and Ω is the generator's mechanical speed.

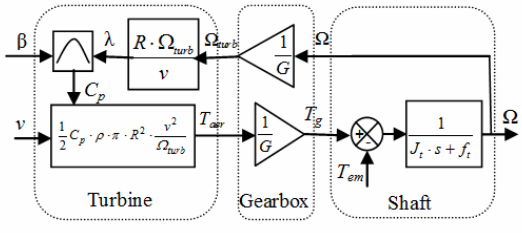

Fig. 3 – Block diagram of the wind turbine model.

The system of equations (11) to (14) permits to us to construct the block diagram of the wind turbine model as shown in Fig. 3, where G is the gear ratio and T_{aer} is the aerodynamic torque.

5. MAXIMUM POWER POINT TRACKING TECHNIQUE

The characteristics of the power coefficient $C_p(\lambda)$ for different values of the pitch angle β are illustrated in Fig. 4.

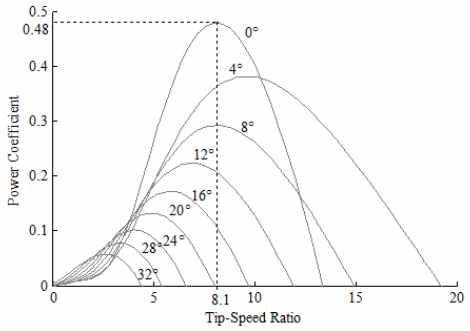

Fig. 4 – Power coefficient versus tip-speed ratio for different values of the pitch angle.

We can notice that for a given β, there is one value of λ noted λ_{opt} for which C_p is maximum.

In addition, when $\beta = 0$, the turbine is most efficient ($C_{p\max} = 0.48$ and $\lambda_{opt} = 8.1$).

According to (12), we can see that if the rotor speed Ω_{turb} is kept constant, then any change in the wind speed will change the tip-speed ratio λ, leading to degrade the power coefficient C_p, as well as the output generated power of the wind turbine.

However, if the rotor speed is adjusted according to the wind speed variations, then the tip-speed ratio can be maintained at its optimal point λ_{opt}, thus C_p at its maximum value C_{pmax} which could yield maximum output power from the system according to (11). So the MPPT technique consists in varying the wind turbine speed constantly according to the wind speed variations, so that the tip-speed ratio is maintained in its optimum value, so that the power generation is optimum.

5.1. MPPT CONTROL SCHEME

In order to extract the maximum power from the wind, we adopted the speed control strategy. It permits to carry the speed of the wind turbine into the desired value which corresponds to the maximum power point. The control scheme of the rotor speed using a linear controller (C_Ω) is represented in Fig. 5. The control structure consists in adjusting the torque appearing on the turbine shaft in order to fix the wind turbine speed at a reference which permits to track the maximum of the wind power. This reference is deducted from (12). Using the gear ration G, we obtain:

$$\Omega_{ref} = \frac{\lambda_{opt} \cdot v \cdot G}{R}. \tag{15}$$

Since the aerodynamic torque T_{aer} thus T_g is a nonlinear function of Ω, its compensation permits the linearization of the process associated at its control. As a result, the synthesis of the controller is found largely simplified.

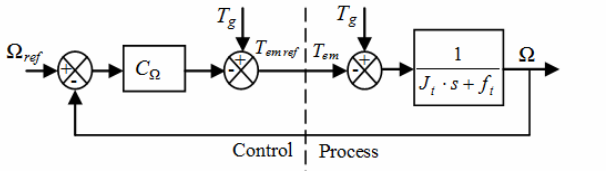

Fig. 5 – Control scheme of the rotor speed for MPPT.

However, the compensation of the term which causes the nonlinearity of the system is just an approach which could a little discard the real system of its control. To approach more to the reality, we have developed a nonlinear algorithm to control the rotor speed which takes into account the nonlinearity of the system. In addition, the wind speed which is variable and unpredictable is considered as a perturbation for our system. Therefore, we need a robust control algorithm which permits the system to reach its reference without being affected by this perturbation.

5.2. SLIDING MODE CONTROL TECHNIQUE

The sliding mode control is one of the nonlinear techniques. It is a particular operation mode of variable structure control systems. Its concept consists in moving the state trajectory of the system to a predetermined surface called sliding surface and maintaining it around this latter with a proper switching logic [6, 10].

In general, for a system defined by the state equation (16), for a vector $\boldsymbol{u}$ of dimension m, we must choose m surfaces.

$$\dot{\boldsymbol{x}} = f(x) + g(x) \cdot \boldsymbol{u}, \tag{16}$$

with $\boldsymbol{x} \in R^n$; $\boldsymbol{u} \in R^m$.

Concerning the surface form, the following form is proposed [11 pp. 277–286]:

$$S(x) = \left(\frac{\mathrm{d}}{\mathrm{d}t} + \delta \right)^{\alpha - 1} \cdot e(x), \tag{17}$$

with: $e(x)$ – the error between the variable and its reference; δ – positive constant indicating the desired control bandwidth; α – relative degree, equal to the number of times to derive the output to appear the command.

When the control system operates in variable structure sliding mode, the switching law always respects the condition: $S(x) = 0$. Therefore, the derivative versus time should also always be zero, *i.e.* $\dot{S}(x) = 0$.

In order to respect this condition all times known as the "existence condition", the control law should take a well determined value, designated by the "equivalent control" u_{eq}. Furthermore, in order to lead the evolution trajectory of the system to $S(x) = 0$, the system must be submitted to the attraction of this surface. This will be done by the "attractive control" u_a determined by the "condition of attractiveness":

$$S(x) \cdot \dot{S}(x) < 0. \tag{18}$$

The attractive control u_a defines the dynamic behavior of the system during the trajectory convergence mode to the sliding surface. It is equal to zero once the sliding mode is achieved. The simplest solution is to choose u_a with the relay shape:

$$u_a = -k \cdot \mathrm{sgn}\left[S(x) \right], \tag{19}$$

with $k > 0$ and sgn(.) is the signum function.

Thus the necessary control law to bring back the variable we want control to the selected surface, respecting both existence and attractiveness conditions, is given by:

$$u = u_{eq} + u_a \,. \tag{20}$$

5.3. SLIDING MODE CONTROL ALGORITHM OF THE ROTOR SPEED

To design a sliding mode speed controller, we consider the equation system (21):

$$\dot{\Omega} = \frac{1}{J_t}\left(T_g - T_{em} - f_t \cdot \Omega\right). \tag{21}$$

We choose the error as being the sliding surface:

$$S(\Omega) = e(\Omega) = \Omega_{ref} - \Omega \,. \tag{22}$$

This surface derivative is:

$$\dot{S} = \dot{\Omega}_{ref} - \dot{\Omega} \,. \tag{23}$$

To ensure the attractiveness condition (eq. (18)), $\dot{S}$ is chosen as follow:

$$\dot{S} = -k_1 \cdot \mathrm{sgn}(S) - k_2 \cdot S \,, \tag{24}$$

where k_1 and k_2 are positive constants, sgn(S) is the signum function.

So, the control law ($T_{em\,ref}$) can be obtained from eq. (21–24) as follow:

$$T_{emref} = J_t\left(-k_1 \cdot \mathrm{sgn}(S) - k_2 \cdot S - \dot{\Omega}_{ref}\right) + T_g - f_t \Omega \,. \tag{25}$$

k_1 and k_2 are chosen so that to have satisfactory overshoot and response time.

The sliding mode control scheme of the rotor speed seeking the MPPT is represented in Fig. 6.

6. PITCH CONTROL ALGORITHM

When the wind speed is above the nominal value, the control objective is to maintain the output power constant by means of the blade pitch angle control.

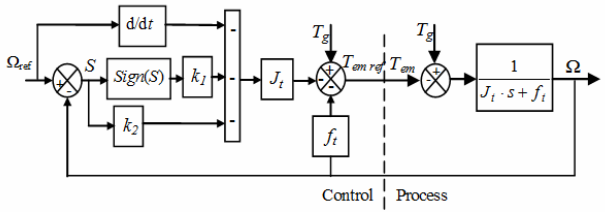

Fig. 6 – Sliding mode control scheme of the rotor speed.

However, the pitch angle is not able to reach the set point value immediately. Accordingly, a rate limiter is implemented in the pitch controller model [12].

In this paper, the maximum pitch angle rate is set at 10°/s (degrees/second). The configuration based on a closed loop structure with a saturation of the pitch angle and the limitation of its rate has been adopted here. The required pitch angle is generated by a proportional-integral (PI) power controller to regulate the power to the rated value.

The pitch angle control scheme is represented in Fig. 7.

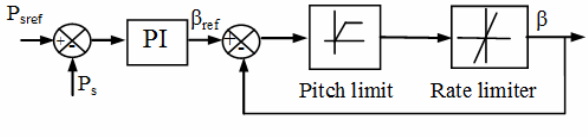

Fig. 7 – Pitch angle control block diagram.

7. SIMULATION RESULTS

The simulation is carried out using the Matlab/Simulink software. The wind turbine parameters are given in Table 1.

Figure 8 shows the wind speed used in this simulation. The simulation results are presented in Figs. 9–14. They show the performances of the wind turbine output power control with both the MPPT technique using a sliding mode speed controller (operating in the partial load region) and the pitch controller associated to operate in full load region.

The sliding mode controller has permitted to extract the maximum of power from the wind. Fig. 9 shows that the generator speed follows its reference successfully with rapid response. When Fig. 10 shows the sliding mode surface equals to zero ensuring that the sliding mode controller parameters have been properly chosen.

In Fig. 11, we can see that the reactive power follows perfectly its reference imposed to be zero, to guarantee the unit power factor of output power in stator side.

Figure 12 indicates that the average value of the dc bus voltages follows perfectly its reference set at 350 V, which assure a good behavior of the grid side converter.

Figure 13 shows the active power and the power coefficient responses before including the pitch control. This later is here maintained at zero (the value for which the power coefficient is at its maximum). So Fig. 13a indicates that the generator's active power follows its reference perfectly. This reference is provided by the speed control system to maximize the generated power. We can see that the generated power exceeds the rated value (4 kW) when the wind speed takes values over (7 m/s). Concerning the power coefficient (Fig. 13b), it reaches the optimal value ($C_{p\max} = 0.48$) which guarantees the MPPT operation.

Figure 14 shows the generator active power (a), the power coefficient (b) and the pitch angle (c) responses when the pitch control is carried out. This later operates at the moments when the wind speed is above the threshold which is in our case (7 m/s) in order to maintain the output power in its rated value. So the pitch angle is controlled to zero in maximum power region and to a positive value in constant power region. As we can see in Fig. 14b, the power coefficient is degraded when the pitch angle increases; this action is justified by Fig. 4. Actually, in this case, we are no more concerned by the MPPT, but rather by maintaining constant the generated power for system protection.

Table 1

Wind turbine parameters

Rated power (kW)	4
Air density (kg/m^3)	1.225
Radius of rotor (m)	3
Gear ratio	5.4
Total inertia (kg.m^2)	0.2

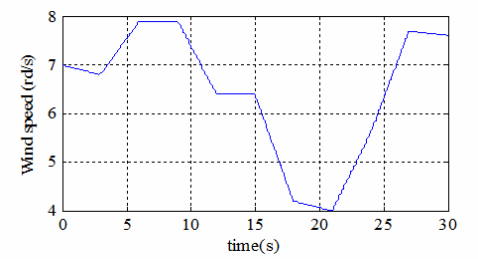

Fig. 8 – Wind speed profile.

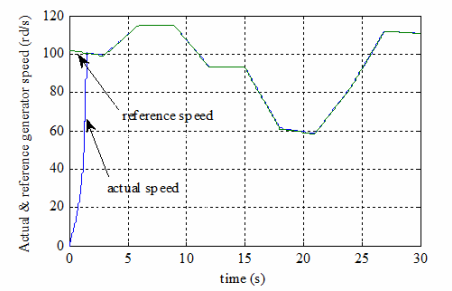

Fig. 9 – Actual and reference generator speed.

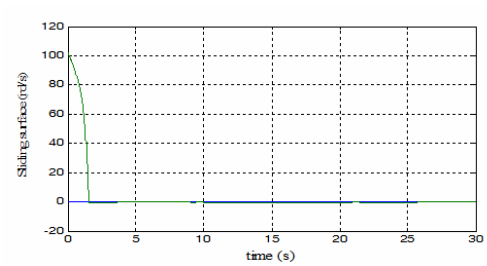

Fig. 10 – Sliding surface for speed regulation.

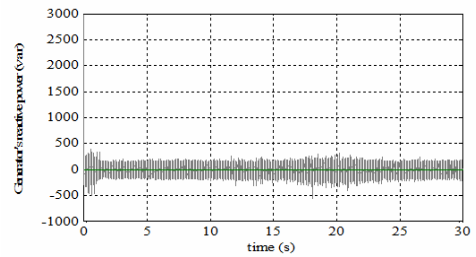

Fig. 11 – Actual and reference generator's reactive power.

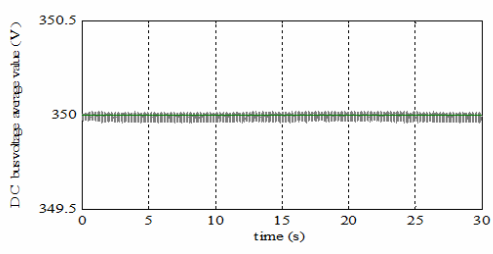

Fig. 12 – Dc bus voltages average value.

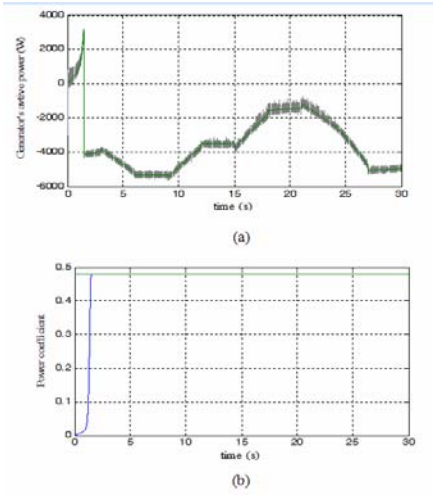

Fig. 13 – performances of the wind turbine without the pitch control: a) actual and reference generator's active power;
b) power coefficient.

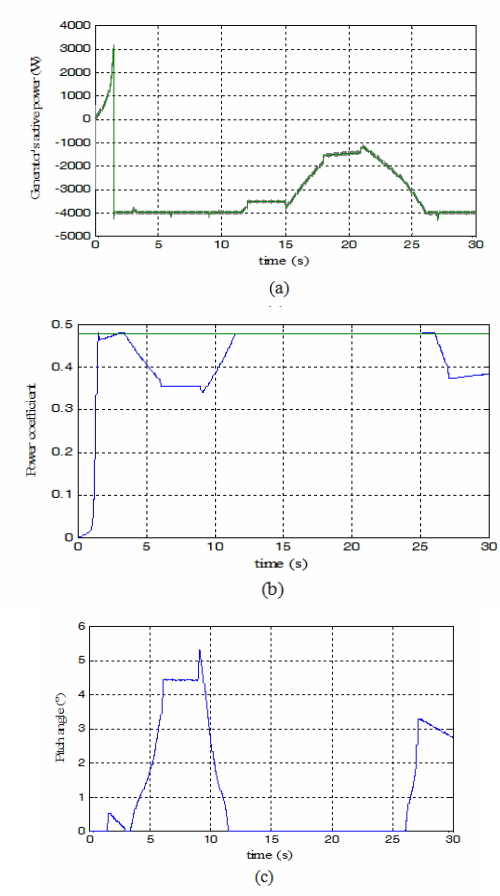

Fig. 14 – Performances of the wind turbine with the pitch control:
a) actual and reference generator's active power;
b) power coefficient; c) pitch angle evolution.

8. **CONCLUSIONS**

In this paper, a variable wind energy conversion system based on a DFIG has been studied. The whole system has been controlled so that the generated power is optimal. For that, we have proposed a MPPT control strategy based on the control of the rotor speed using a sliding mode algorithm. The

vector control based on the stator flux orientation applied to the generator has permitted to separately control the active and reactive generated powers.

A pitch angle controller has been added to regulate the electric power to its rated value in above rated wind speed regime.

The simulation results clearly show that the nonlinear controller successfully controls the wind turbine speed, satisfying static and dynamic performances, which confirms the effectiveness of the sliding mode technique in terms of maximization of the extracted power. In addition, the pitch control system has allowed a secured operation of the wind turbine.

Finally, we can say that the simulation results have shown a good behavior of the conversion system in all wind speed regimes.

Received on February 18, 2016

REFERENCES

1. O. Barambones, P. Alkorta, M. De La Sen, *Wind turbine output power maximization based on sliding mode control strategy*, Proc. of 2010 International Symposium on Industry Electronics (ISIE), Bari, Italy, July 2010, pp. 364–369.
2. B. Beltran, M.E.H. Benbouzid, T. Ahmed-Ali, *High-order sliding mode control of a DFIG–based wind turbine for power maximization and grid fault tolerance*, Proc. of IEEE International Conference of Electric Machines and Drives (IEMdc), Miami, FL USA, May 2009, pp.183–189.
3. G. Tapia, A. Tapia, *Wind generation optimization algorithm for a doubly fed induction generator*, IEE Proc. – Gener.Transm. Distrib. **152**, *2*, pp. 253–263 (2005).
4. X. Zheng, L. Li, D. Xu, J. Platts, *Sliding mode MPPT control of variable speed wind power system*, Proc. of Asia–Pacific Power and Energy Engineering Conference (APPEEC), Wuhan, China, March 2009, pp. 1–4.
5. A. Aberbour, K. Idjdarene, Z. Boudries, *Adaptable sliding mode control for wind energy application*, Rev. Roum. Sci. Techn. – Electrotechn. Energ., **61**, *3*, pp. 258–262 (2016).
6. K. Boulâam, A. Boukhelifa, *Fuzzy sliding mode control of DFIG power for a wind conversion system,* Proc. of 16th International Power Electronics and Motion Control Conference and Exposition (PEMC), Antalya, Turkey, Sept. 2014, pp. 353–358.
7. T. Pan, Z. Ji, Z. Jiang, *Maximum power point tracking of wind energy conversion systems based on sliding mode extremum seeking control*, Proc. of IEEE Energy 2030, Atlanta, GA USA, Nov. 2008, pp. 1–5.
8. M. Adjoudj, M. Abid, A. Aissaoui, Y. Ramdani, H. Bounoua, *Sliding Mode Control of a Doubly Fed Induction Generator for Wind Turbines*, Rev. Roum. Sci. Techn. – Electrotechn. Energ., **56**, *1*, pp. 15–24 (2011).
9. Y. Cheng, C. Qian, M.L. Crow, S. Pekarek, S. Atcity, *A Comparison of Diode-Clamped and Cascaded Multilevel Converters for a STATCOM With Energy Storage*, IEEE Transactions on Industrial Electronics, **53**, *5*, pp. 1512 – 152 (2006).
10. V.I. Utkin, *Sliding mode control design. Principles and applications to electric drives*, IEEE Trans. on Industrial Electronics, **40**, *1*, pp. 23– 36, (1993).
11. J.J.E. Slotine, W. Li, *Applied nonlinear control*, Prentice-Hall, Englewood Cliffs, NJ USA, 1991, pp. 277–286.
12. M. Cirrincione, M. Pucci, G. Vital, *Neural MPPT of variable pitch wind generators with induction machines in a wide wind speed range*, IEEE Transactions on Industry Applications, **49**, *2*, pp. 942–953 (2013).